The Journal of Antibiotics (2018) 71:713–721
https://doi.org/10.1038/s41429-018-0056-9

JARA Japan Antibiotics Research Association
The Society for Actinomycetes Japan

ARTICLE

Cationic amphiphilic bolaamphiphile-based delivery of antisense oligonucleotides provides a potentially microbiome sparing treatment for *C. difficile*

Arun K. Sharma[1] · Jacek Krzeminski[1] · Volkmar Weissig[2] · John P. Hegarty[3] · David B. Stewart[4]

Received: 27 February 2018 / Revised: 27 March 2018 / Accepted: 29 March 2018 / Published online: 19 April 2018

Abstract

Conventional antibiotics for *C. difficile* infection (CDI) have mechanisms of action without organismal specificity, potentially perpetuating the dysbiosis contributing to CDI, making antisense approaches an attractive alternative. Here, three (APDE-8, CODE-9, and CYDE-21) novel cationic amphiphilic bolaamphiphiles (CABs) were synthesized and tested for their ability to form nano-sized vesicles or vesicle-like aggregates (CABVs), which were characterized based on their physiochemical properties, their antibacterial activities, and their toxicity toward colonocyte (Caco-2) cell cultures. The antibacterial activity of empty CABVs was tested against cultures of *E. coli*, *B. fragilis*, and *E. faecalis*, and against *C. difficile* by "loading" CABVs with 25-mer antisense oligonucleotides (ASO) targeting *dnaE*. Our results demonstrate that empty CABVs have minimal colonocyte toxicity until concentrations of 71 μM, with CODE-9 demonstrating the least toxicity. Empty CABVs had little effect on *C. difficile* growth in culture (MIC90 ≥ 160 μM). While APDE-8 and CODE-9 nanocomplexes demonstrated high MIC_{90} against *C. difficile* cultures (>300 μM), CYDE-21 nanocomplexes demonstrated MIC_{90} at CABV concentrations of 19 μM. Empty CABVs formed from APDE-8 and CODE-9 had virtually no effect on *E. coli*, *B. fragilis*, and *E. faecalis* across all tested concentrations, while empty CYDE-21 demonstrated MIC_{90} of >160 μM against *E. coli* and >40 μM against *B. fragilis*and *E. faecalis*. Empty CABVs have limited antibacterial activity and they can deliver an amount of ASO effective against *C. difficile* at CABV concentrations associated with limited colonocyte toxicity, while sparing other bacteria. With further refinement, antisense therapies for CDI may become a viable alternative to conventional antibiotic treatment.

Introduction

C. difficile infection (CDI) is the most frequently reported nosocomial bacterial infection [1] in the United States, accounting for more than 450,000 new cases annually and for more than four billion dollars in CDI-attributable annual health care costs [2]. CDI has a strong reliance on intestinal dysbiotic states, which, when combined with the presence of *C. difficile* in the human gut, represents the most common pathogenesis for CDI. The high prevalence of this infection is, in large part, due to formidable recurrence rates of 15–25% following first treatment [3] with conventional antibiotics (CAs). CAs have long been recognized as the most important risk factor for the development of CDI [4], due to their mechanisms of action lacking organismal specificity, leading to widespread changes in gut ecology [5], which can lead to CDI by disrupting the gut microbial community. Given the important role of intestinal dysbiosis in the development of CDI, there has also been recent interest in studying the effects of *difficile*-directed conventional antibiotics on the bacterial and fungal communities of human subjects being treated for CDI, as a way of potentially explaining the high persistence and recurrence rates of this disease. These more recent data [6] suggest that even

✉ David B. Stewart
dbstewart@surgery.arizona.edu

1 Department of Pharmacology, College of Medicine, The Pennsylvania State University, Hershey, PA 17033, USA

2 Department of Pharmaceutical Sciences, Nanomedicine Center of Excellence, College of Pharmacy Midwestern University, Glendale, AZ 85308, USA

3 Department of Medicine, College of Medicine, The Pennsylvania State University, Hershey, PA 17033, USA

4 Department of Surgery, University of Arizona – Banner University Medical Center, Tucson, AZ 85724, USA

difficile-directed conventional antibiotics could potentially contribute to the perpetuation of dysbiotic states, which in turn could perpetuate CDI, potentially leading to even primary treatment failures.

There has been previous [7, 8] interest in the development of antisense therapies to treat bacterial infections, in part due to concerns regarding antibiotic resistance to traditional drugs. Given the dependence of CDI on dysbiotic states, approaches using therapeutic antisense oligonucleotides (ASO) complimentary to specific *C. difficile* mRNAs could limit or prevent the expression of important bacterial genes leading to bacterial death, all while sparing other organisms. This approach would offer significant advantages over CAs, especially in terms of a more limited impact on gut microbial communities. Developing clinically effective antisense therapies targeting a Gram-positive organism requires several elements. Since antisense oligonucleotides will not be efficiently introduced into bacteria without assistance given the presence of both a cell membrane and a thick cell wall, a carrier molecule must be used to deliver the ASO. This carrier must complex with the ASO strongly enough to concentrate it, to protect it from degradation in the extracellular environment, and to focus its delivery on its target cell. In order to accomplish these activities, the carrier-ASO complex itself must be stable in the in vivo environment of the gut. Once at the cell, the carrier must be able to release its cargo. Simultaneously, the carrier must demonstrate both limited gut toxicity and limited antibacterial activity at the doses required to effectively treat the target bacteria.

Our group published the first [9] in vitro data for antisense therapies against CDI by complexing cyclohexyl dequalinium analogs to various ASO-targeting essential *C. difficile* genes. However, since dequalinium has both antibacterial activity as well as toxicity at higher doses, a better delivery compound for ASO is required if antisense approaches to CDI are to be further developed. Here, we report our data on vesicles formed from novel cationic amphiphilic bolaamphiphiles (CABs) as carriers for chimeric 25-mer 2′-*O*-methyl phosphorothioate ASO. CABs, characteristic of all bola-like compounds, have hydrophilic, positively charged end groups separated by a hydrophobic linker chain. This molecular structure enables CABs to form nano-sized vesicle-like aggregates (CABVs), which in turn allow them to complex with negatively charged oligonucleotides in addition to promoting electrostatic interactions with bacterial cell membranes for intracellular delivery of ASO. The synthesis, physiochemical properties, toxicity, and antibacterial properties of three novel CABs and their respective CABVs are described, and their specificity for *C. difficile* compared to several other organisms is also provided.

Materials and methods

This work was performed with approval from the Pennsylvania State Milton S. Hershey Medical Center Institutional Review Board (IRB). *C. difficile* samples were obtained from a previously described [10] IRB-approved tissue bank of the senior author (DS), which contains deidentified, patient-derived glycerol stocks of *C. difficile* previously genetically characterized by our team, including designation of ribotype. Stocks of *Escherichia coli* (ATCC 25922), *Bacillus fragilis* (ATCC 25285), and *Enterococcus faecalis* (ATCC 29212*E*) were provided by the Penn State Clinical Microbiology laboratory.

Bacterial strains and growth conditions

A *C. difficile* ribotype 027 isolate (HMC083) was cultured on CDC anaerobe 5% sheep blood/phenylethyl alcohol agar, while *E. coli*, *B. fragilis*, and *E. faecalis* were cultured on Trypticase soy agar with 5% sheep blood (TSA II; BD Diagnostics). For anaerobic organisms, cultures were incubated under anaerobic incubation (85% N_2, 10% CO_2, 5% H_2; Anoxomat, Advanced Instruments, Inc., Norwood, MA, USA) at 37 °C.

Synthesis and purification of bolaamphiphile compounds *N,N′*-(Decane-1,10-diyl)bis(4-aminopyridinium)dichloride (APDE-8)

A mixture of 4-aminopyridine (1.5 g, 15.9 mmol) and 1,10-dichlorodecane (1.61 g, 7.95 mmol) in amyl alcohol (26 mL) was stirred and refluxed under N_2 for 21 h. After cooling to room temperature, white precipitate formed was filtered off and washed with acetone/water to yield 2.4 h (75%) of APDE-8, which was further purified by crystallization from ethanol [Mp 278–282 C. ^{1}H NMR (500 MHz, DMSO-d_6) δ 1.17–1.26 (m, 12 H), 1.70–1.75 (m, 4 H), 4.10 (t, 4 H, $J = 6.0$ Hz), 6.87 (d, 4 H, $J = 6.5$ Hz), 8.20 (d, 4 H, $J = 6.0$ Hz), 8.23 (s, 4 H, NH_2). MS *m/z* 327.1565 $(M\text{-}2Cl)^+$].

N,N′-(Decane-1,10-diyl)bis(2,4,6-trimethylpyridinium)dibromide (CODE-9)

A mixture of 2,4,6-trimethylpyridine (4.8 g, 39.6 mmol) and 1,10-dibromodecane (5.4 g, 18.0 mmol) was heated at 180–195 °C for 3 h. After that time almost all material solidified into crystalline brown mass. This material was stirred with a methanol/ether mixture and filtered. The filtrate was concentrated in vacuo and chromatographed on aluminum oxide column using 1% methanol in methylene chloride as an eluent to yield 0.7 g (72%) of CODE-9, which was crystallized from a mixture of methanol and

diethyl ether [Mp 190–192 °C (dec). ^{1}H NMR (500 MHz, DMSO-d_6) δ 1.27–1.38 (m, 8 H), 1.41–1.46 (m, 4 H), 1.73–1.79 (m, 4 H), 2.49 (s, 6 H, 2 × CH_3), 2.81 (s, 12 H, 4 × CH_3), 4.39 (t, 4 H, $J = 7.0$ Hz), 7.76 (s, 4 H). MS *m/z* 381.2267 $(M\text{-}2Br)^+$].

N,N′-(Decane-1,10-diyl)bis(9-amino-2,3-dihydro-1*H*-cyclopenta[b]quinolinium)dichloride (CYDE-21)

A mixture of 2,3-dihydro-1*H*-cyclopenta[b]quinolin-9-ylamine (0.45 g, 2.44 mmol), 1,10-dichlorodecane (0.25 g, 1.2 mmol), and sulfolane (2 mL) was heated at 190–200 °C for 90 h. The resulting mass was stirred with methanol and filtered. The filtrate was concentrated and chromatographed on an Al_2O_3 column using a gradient from 1 to 25% of methanol in methylene chloride. Fractions containing required product were pooled together and evaporated, and the resulting off-white solid (31 mg, 4.5%) was further purified by crystallization from a methanol/acetone mixture [Mp 250–258 °C (dec). ^{1}H NMR (500 MHz, $CDCl_3$) δ 1.27–1.43 (m, 12 H), 1.67–1.76 (m, 4 H), 2.20–2.26 (m, 4 H), 2.95 (t, 4 H, $J = 7.5$ Hz), 3.38 (t, 4 H, $J = 7.5$ Hz), 3.63 (t, 4 H, $J = 7.0$ Hz), 4.46 (t, 4 H, $J = 6.5$ Hz), 7.72 (t, 2 H, $J = 7.0$ Hz), 7.98 (t, 2 H, $J = 7.5$ Hz), 8.15 (d, 2 H, $J = 9.0$ Hz), 8.54 (d with fine splitting, 2 H, $J = 8.5$ Hz), 8.92 (br s, 4 H, NH_2).

Purity determination of CABs

The purity of the compounds was determined by analytical HPLC using a Zorbax SB-C8 3.0 mm × 25 cm column. Isocratic elutions using solvent mixtures of A = water + 0.5% sodium hexanesulfonate + 0.5% orthophosphoric acid, and $B = CH_3OH$ + 0.5% sodium hexanesulfonate + 0.5% orthophosphoric acid at a ratio of A:B/25:75 and at a rate of 1 ml/min were performed; the compounds were found to be ≥98% pure.

Characterization of CABVs

CABVs were prepared as previously [9] described. Briefly, all compounds were dissolved in a round-bottom flask using between 2 and 10 mL of methanol followed by removal of the solvent using a rotary evaporator. The remaining thin-film residue was hydrated with ultrapure water at a final concentration of 10 mM, resulting either in a suspension (CODE-9 and CYDE-21) or a slightly opaque solution (APDE-8). The opaque solution was immediately examined for the presence of spontaneously formed vesicles via dynamic light scattering (DLS) using a Zetasizer Nano series instrument from Malvern Instruments (Westborough, MA, USA). The suspensions were probe sonicated on ice via pulse sonication for 45 min followed by centrifugation for 10 min at 3000 × *g* to remove any undissolved solid material. The supernatant was collected and examined for the presence of nano-sized vesicles (CABVs). All sample preparations were analyzed in triplicate.

dnaE sequence analysis

As previously described [9], prior whole genome shotgun sequencing of a tissue-banked ribotype 027 *C. difficile* isolate performed by our group using Illumina MiSeq provided sequences for the 5′-UTR of *dnaE*, a DNA polymerase III alpha subunit important for DNA replication. Using NCBI BLAST, sequences were selected which were specific to *C. difficile* and which targeted accessible local secondary mRNA structures near start codons, while also selecting sequences predicted in silico to minimize off-target effects. Therefore, this ASO was selected for use in the present study due to its specificity to *C. difficile* and to due to its previous effectiveness in treating *C. difficile* in culture. The ASO (Integrated DNA Technologies, Coralville, IA, USA) sequence was identical to one previously described [9].

Testing CABV-binding capacity

CABV complexation of 25-mer phosphorothioate gapmer oligonucleotides was determined using an Oligreen (Thermo Fisher Scientific, Wilmington, DE, USA) unsymmetrical cyanine dye exclusion assay. Binding was measured by exclusion of dye from oligonucleotide binding through triplicate testing of serial doses of CABVs with 2 µg/mL gapmer ASO solutions placed in black 96-well optical bottom microplates (Nunc; Thermo Fischer Scientific, Wilmington, DE, USA). Each CAB was suspended in DMSO to a concentration of 20 mg/mL, preparing 1× and 10× working solutions of CABVs seeded in dilute water. Each solution was sonicated on ice for 30 min with a high-intensity probe using 30 s on/off cycles at 25% amplitude with a power setting of 6 W.

A working dilution was then prepared with 150 µL Oligreen added to 150 µL 200× TE and 15 µL of nfH20. Scrambled 25-mer gapmer stocks (1 mM) were suspended in 46.3 µL of 10 mM Tris-HCL (ph 8.0), preparing 50 µM gapmer working dilutions; 5 µL of this solution was added to separate triplicate well sets in 3× 96-well plates, with the addition of both 1× and 10× CABV solutions added to gapmer solutions to accomplish a stepwise mixing of CABVs. Following a 20-min incubation period to stabilize the fluorescence signal, fluorescent readings (485 nm excitation, 520 nm emission; 20 nm bandwidth) were recorded and complexation curves were created.

Testing of empty CABV toxicity on Caco-2 cell lines

Determination of colonocyte viability was assessed using a Vialight™ Plus Cytotoxicity Assay (Lonza; Allendale, NJ, USA). Monolayers of Caco-2 cells were cultured in T-170 flasks to 80% confluence, seeding cells on 96-well plates (2×10^5 cells/well). Cells were incubated to confluence over 48 h, and were exposed to empty CABVs for 24 h, with CABV-untreated Caco-2 cells used as a control. Thereafter, 50 µL of cell lysis reagent was added to each well. After 15 min on an orbital shaker, 100 µL of cell lysates were transferred to white-walled chimney plate wells, and 100 µL of ATP monitoring reagent was added to each well, with a 2-min incubation period in the dark. Plates were then read using a spectrophotometer, using a luminescence program with 1 s integration times (570 nm emission).

Testing of empty CABVs and loaded CABV nanocomplexes against bacteria

Empty CABVs as well as CABVs loaded with 25-mer ASO targeting the *C. difficile dnaE* gene were tested against *C. difficile*. Additionally, empty CABVs were also tested against *E. coli*, *B. fragilis*, and *E. faecalis*. Using BHI-S, a broth microdilution method was used to determine the lowest concentration of empty CABV or CABV–ASO nanocomplex to achieve MIC_{90} after 24 h of exposure. Growth of bacteria was assessed at OD_{630} using a spectrophotometer, comparing treated cultures where growth is inhibited (<0.1 log growth) to the OD_{630} values of the initial inoculum, from which MIC_{90} values were calculated (equivalent to an OD_{630} of 0.08) [11, 12].

Results

Synthesis of CABs

The CABs APDE-8, CODE-9, and CYDE-21 were synthesized by modification of the previously reported methods [13] as shown in Fig. 1. APDE-8 was synthesized by refluxing 4-aminopyridine and 1,10-dichlorodecane in amyl alcohol. CODE-9, on the other hand, was obtained by heating a mixture of 2,4,6-trimethylpyridine and 1,10-dibromodecane in the absence of solvent. CYDE-21 was synthesized by heating 2,3-dihydro-1*H*-cyclopenta[b]quinolin-9-ylamine and 1,10-dichlorodecane in the presence of sulfolane for 90 h. The compounds were purified by crystallization or column chromatography on alumina followed by crystallization, and they were characterized on the basis of ^{1}H NMR and high-resolution MS data. The purity of the compounds as confirmed by analytical HPLC was found to be ≥98%.

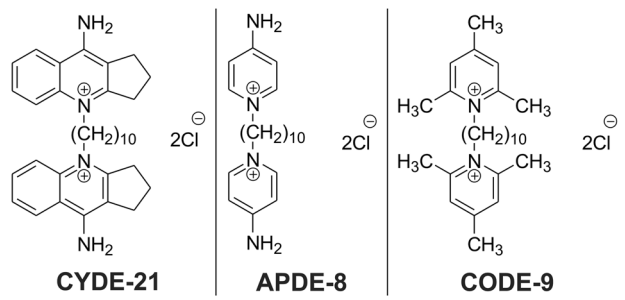

Fig. 1 Structure of three novel cationic amphiphilic bolaamphiphiles (CYDE-21, APDE-8, and CODE-9)

Table 1 Physiochemical testing for empty cationic amphiphilic bolaamphiphile vesicles

Compound	Peak size (nm)	St. dev. (nm)	PdI	Zeta potential (mV)	St. dev (mV)
APDE-8	186	57	0.282	13.9	5.35
	191	49	0.252	11.5	6.36
	202	66	0.226	10.4	5.03
CYDE-21	449	169	0.428	51.3	10
	480	233	0.437	55	8.57
	433	159	0.450	57.5	11.2
CODE-9	143	21	0.651	21.4	4.56
	169	28	0.614	21.1	5.71
	123	18	0.738	20.8	9.02

nm nanometer, *St. dev.* standard deviation, *PdI* polydispersity index

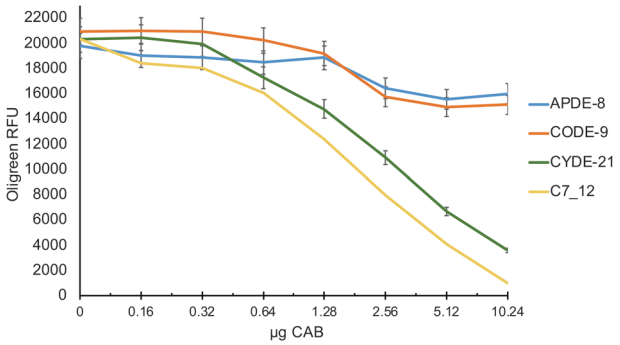

Fig. 2 Dose-complexation curves for CAB-binding capacities based on Oligreen dye exclusion. The *y*-axis provides relative fluorescence units (RFU) and *x*-axis provides microgram amount of CABV

Physiochemical characterization of CABVs

Table 1 provides a description of peak size, dispersity, and the zeta potential for each CABV. Figure 2 provides dose-complexation curves created to assess CABV-binding capacities based on Oligreen dye exclusion. After adjusting for background fluorescence, CABVs formed from APDE-8 and CODE-9 were found to have weak dye exclusion, while CABVs formed from CYDE-21 reached

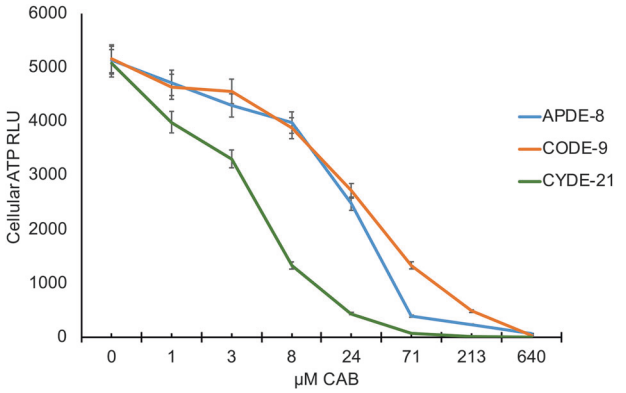

Fig. 3 Dose effects of empty CABVs on Caco-2 toxicity. The *y*-axis defines intracellular ATP levels assessed by relative luminosity units (RLU) and the *x*-axis provides micromolar concentrations of CABVs

50% gapmer complexation at a weight amount of 4 μg. As a reference, vesicles made from a cyclohexyl dequalinium analog (10-cyclohexyl-DQA) described in previous work by our group [9] achieved 50% gapmer complexation at a weight amount of 2 μg CAB.

Cytotoxicity of Caco-2 cells to empty CABVs

Figure 3 provides dose effects of empty CABVs on Caco-2 monolayers, assessing for Caco-2 toxicity based on cellular ATP levels. A ≥90% reduction in luminescence was observed at a concentration of 71 μM with APDE-8, at 213 μM of CODE-9, and at 24 μM of CYDE-21.

Exposure of bacteria to empty CABVs

Figure 4 provides results of *C. difficile* growth in response to varying doses of each CABV. APDE-8-based CABVs demonstrated virtually no effect on *C. difficile* growth across all concentrations tested. Vesicles made from CODE-9 demonstrated an MIC_{90} to *C. difficile* of 320 μM, while CYDE-21-based vesicles were noted to have an MIC_{90} of 160 μM.

Figure 5 provides percent growth of non-*C. difficile* bacteria (*E. coli*, *B. fragilis*, and *E. faecalis*) commonly encountered in the human gut. APDE-8 exposure resulted in minimal changes in bacterial growth, with the greatest decrease in growth noted with *E. faecalis* (25% reduction) at the highest tested empty CABV concentration. Similar to APDE-8, empty CABVs with CODE-9 did not demonstrate significant inhibition of bacterial growth until the highest tested concentration, with a 79% reduction in growth of *E. faecalis* and with a 96% reduction in growth of *B. fragilis*. CABVs with CYDE-21 were noted to cause a significant (>90%) reduction in growth of *B. fragilis* and *E. faecalis* at empty CABV concentrations of 80 μM.

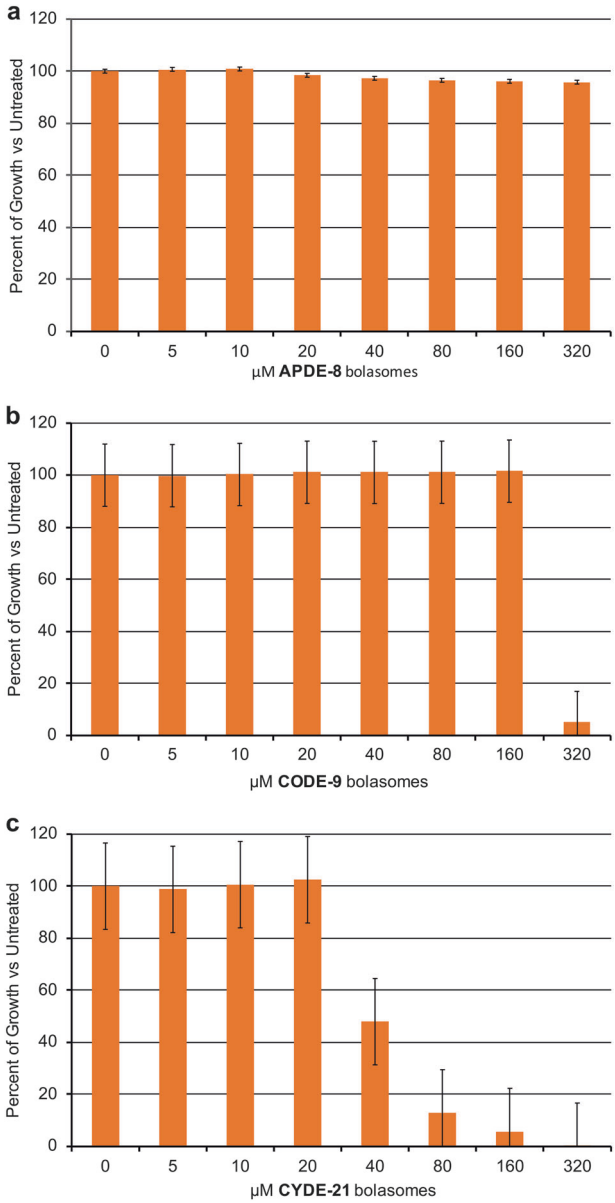

Fig. 4 Percent growth of *C. difficile* treated with empty CABVs using a broth microdilution method

Exposure of bacteria to loaded CABVs (CAB–ASO nanocomplexes)

Figure 6 provides growth inhibition for *C. difficile* in response to varying doses of each CABV nanocomplex. Similar to the performance of their empty versions, APDE-8 nanocomplexes demonstrated virtually no effect on *C. difficile* growth across all concentrations tested, while CODE-9 nanocomplexes demonstrated an MIC_{90} to *C. difficile* of 307 μM. CYDE-21 nanocomplexes were noted to have an MIC_{90} of 19.2 μM.

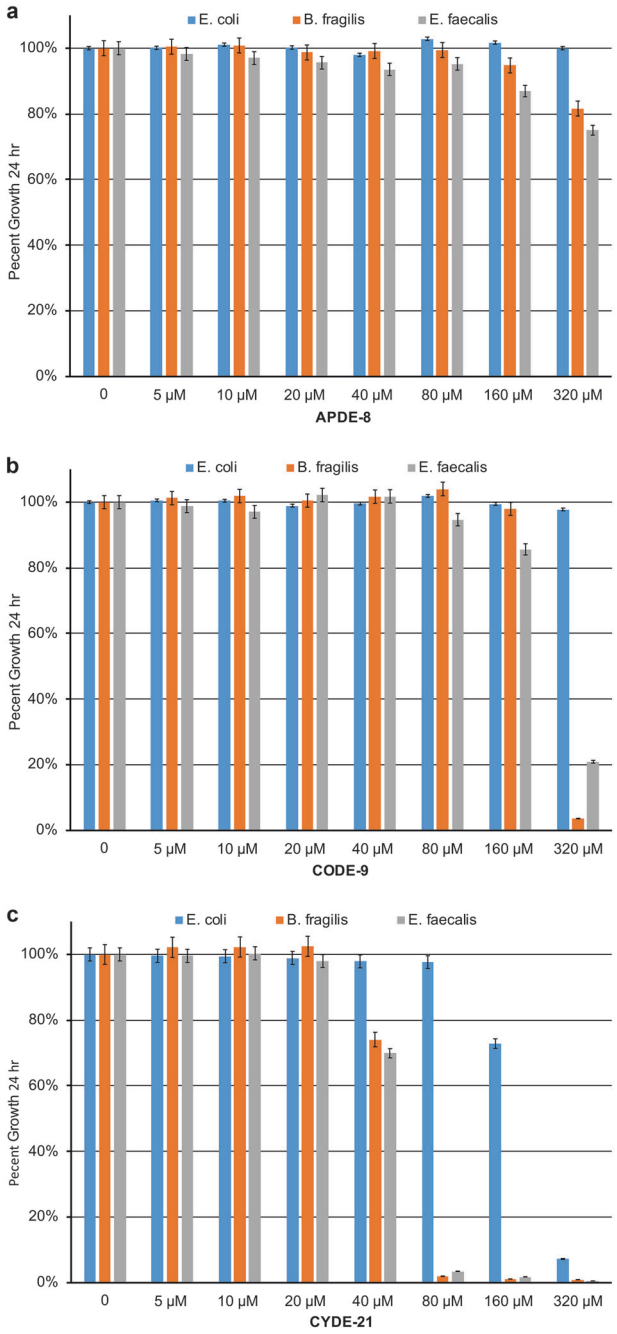

Fig. 5 Percent growth of tested non-*C. difficile* bacteria treated with empty CABVs using a broth microdilution method

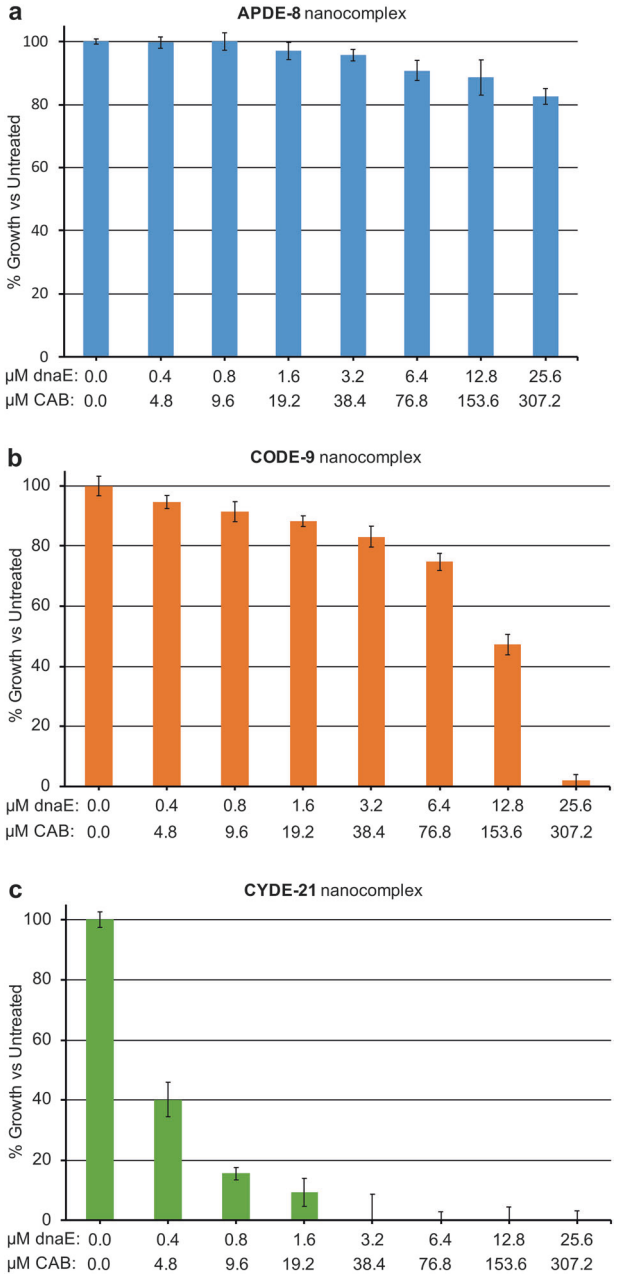

Fig. 6 Percent growth of *C. difficile* treated with CABV–ASO nanocomplexes using a microdilution method. The *y*-axis provides percent growth, and the *x*-axis provides concentrations of both CABVs and the antisense oligonucleotide targeting *dnaE*

Discussion

The current study provides one of the first investigations in the literature proposing an antisense approach to treating *C. difficile*, providing in vitro evidence that CABVs are capable of delivering an effective dose of ASO while limiting toxicity to colonocytes, all with a sparing effect on several non-*C. difficile* bacteria frequently encountered in the human large intestine. While this data is both seminal and preclinical, the concept of a CDI treatment with organismal specificity would represent a significant improvement in disease treatment given the strong role that intestinal dysbiosis has in the pathophysiology of CDI.

The approach to ASO delivery described in this study draws from techniques previously applied to the development of organelle-specific nanocarriers, beginning with the inadvertent discovery that dequalinium chloride could form vesicles useful for delivering mitochondrial-targeted

therapeutics [14, 15]. A high concentration of cardiolipin (CL) within the inner mitochondrial membrane, a distinctive feature of this organelle and a likely reflection of its endosymbiotic evolutionary development, provides a possible explanation for how CABVs deliver ASO to bacteria, as well as informing investigations of structure–activity relationships in the future development of similar novel nanocarriers. CL is a key determinant [16] in the formation of membrane domains in bacteria; its curvature strain promotes CL segregation within regions of the cellular poles and mitotic division sites [17], while its alkyl-bearing head group provides an area of electrostatic compensation with extracellular cationic molecules. Recent work by Marin-Menendez et al. [18] using confocal microscopy of bacterial and liposomal models provided evidence that electrostatic interactions between positive charge centers within nanocarriers and negative charge centers in CL lead to conformational changes within CL-rich bacterial membrane domains, resulting in transient membrane pores which are the likely route of delivery of oligonucleotides into bacterial targets. Cardiolipin is a common phospholipid in the bacterial plasma membrane, and it is unknown if its concentration significantly varies between different bacteria; if it does, this may explain the differential effects that empty CABs had on *C. difficile* and other tested bacteria at higher doses. Electrostatic charge compensation is also a key component to the complexation process between nanocarrier and oligonucleotide; cationic vesicles formed from positively charged bolaamphiphiles must interact strongly enough with an oligonucleotide to form complexes, while permitting decomplexation at the time of delivery. Thus, using a nanocarrier with distinct charge centers has implications for the type of antisense molecules which might participate in stable complexes, making neutral phosphorodiamidate morpholino oligonucleotides, for example, a less desirable alternative ASO for this particular delivery method.

The role that CAs play in initially creating a dysbiotic gut is well established, but the difficulties in reliably curing this infection using drugs with the same broad antibacterial effects as those of the culprit antibiotics represents a significant gap in disease care. Recent work by our group investigating the impact on bacterial and fungal community structures [6] created by *difficile*-directed CAs demonstrated an enrichment of pathogenic bacteria and fungi in response to conventional CDI therapy, with a concomitant enrichment of pro-inflammatory and xenobiotic metabolic pathways based on imputed functional analyses. These changes represent a post-treatment disturbance to the gut environment, one compositionally distinct from the dysbiosis associated with the initial development of CDI. This change to gut microbial communities created by conventional CDI therapy may, ironically, contribute to high persistence and recurrence rates given the organism's strong selective advantage to dominate environmental and metabolic niches [19] frequently created in the setting of CAs.

Antisense therapies offer several advantages beyond greater drug specificity. The production of antisense therapies offers a lower-cost pathway for novel drug development, considering the cost of many modified oligonucleotides. Modification of ASO to address variations in genetic targets is easily accomplished, and ASO potentially allow for therapeutic targets previously unapproachable by conventional antibiotics, including interruption of sporulation and toxin production pathways which would address the major disease reservoir and the principal cause of disease symptoms, respectively. However, the greatest advantage of antisense therapies is organism specificity, a requirement for improved care compared to CAs given the unique relationship between dysbiosis and CDI. Metronidazole and vancomycin are the two most common CAs used to treat CDI, with previously reported [20] MIC_{90} of <4 mg/L for both. In this study, CYDE-21 nanocomplexes yielded an MIC_{90} of 11 mg/L. The best genetic targets will be important enough to bacterial survival that a high transcript copy number will require a large amount of ASO to effect a clinically relevant change in the bacteria, which may explain why CYDE-21 MICs were higher than those for metronidazole and vancomycin. Future studies by our group will evaluate adjustments to the structure of these CABs to further increase the complexation capacity of their corresponding CABVs and to further minimize effects on bacteria and colonocytes attributable to them. The ideal treatment for CDI will involve a balance between efficacy and specificity, with the possibility that a slightly less potent drug with higher levels of specificity than current CAs may represent a superior treatment to current therapy overall. Where these potentially antagonistic goals of efficacy and specificity intersect for maximal treatment benefit will also require further study. Since no current CAs are C. *difficile*-specific, their reliability will be necessarily limited by comparison.

With the release of the most recent guidelines on CDI treatment from the Infectious Diseases Society of America [21], a greater role for the use of fidaxomicin represents a change in how CDI will be treated. Fidaxomicin is a narrow spectrum of activity compared to many other conventional antibiotics, and microbiome studies [22] comparing this drug to vancomycin suggest that it has a lesser impact on gut microbial communities, and that it produces a lesser impact on loss of resistance to *C. difficile* colonization, a phenomenon associated with any conventional antibiotic. Additionally, fidaxomicin is a safe drug, with no higher incidence of mortality or serious adverse events than rates observed [23] with vancomycin. While the drug represents an important advancement in the treatment of CDI, its

availability only as an oral agent limits its usefulness in more severe forms of this infection, where patients may have an ileus or septic shock, preventing the safe and reliable use of orally administered drugs. Intraluminal deliver of antibiotics for CDI, either by enema or via endoscopic delivery, has a particular appeal, applying the drug directly to the affected organ. CABV–ASO complexes are designed with this in mind.

One previously unreported observation from this study is that decreasing mean CABV diameters are associated with increasing MIC_{90} for CABV–ASO nanocomplexes. Based on previous work with dequalinium [9], this trend may indicate that CABVs with smaller diameters form vesicles which are more stable, leading to nanocomplexes that are less likely to release their ASO. This information will be informative for the preparation of new CABVs, and this trend may indicate a possible advantage for larger, bulkier side chains for each cationic head group.

In conclusion, more research into the structure–activity relationship of empty and loaded CABVs and their effect on both bacteria and colonocytes is required to make the approach described here competitive with conventional therapies. The difference in concentrations of empty CABVs causing toxicity in Caco-2 cell cultures (>90% loss) and concentrations of loaded CABVs effectively treating cultures of *C. difficile* (assessed by MIC_{90}) is approximately 3×, and ideally this window would be larger. Further, though continued modification and in vitro testing of loaded CABVs is necessary, success with in vitro testing is not a guarantee of success with subsequent in vivo testing. There is no data on the use of the drugs described herein in a living model (CABs were created de novo, and named, by the authors), and it is unknown if these complexes would be stable in the gut, or whether adequate gut concentrations could be achieved to cure CDI while avoiding toxicity. Nonetheless, this proof-of-concept work suggests that CABVs are a promising nanocarrier for ASO targeting *C. difficile*, with vesicles formed from CYDE-21 delivering 25-mer gapmers in concentrations resulting in growth inhibition of *C. difficile* at concentrations which left tested non-*C. difficile* bacteria largely undisturbed. While some of our CABVs were not effective at ASO delivery, and while CYDE-21-based vesicles demonstrated antibacterial activity at concentrations greater than its MIC_{90} for *C. difficile*, CABV–ASO complexes are a promising platform for effective, organism-specific antibacterial therapy. CDI is associated with an intestinal dysbiosis, and the narrower spectrum of activity of loaded CABVs could potentially improve treatment success by making a small ecological impact on the gut. Additional studies are planned for modifying the structures of these CABVs followed by retesting; eventually, an animal model will be used to evaluate all of our CABVs for toxicity, lethality, and efficacy, while using whole metagenome shotgun sequencing and metatranscriptomic profiling to study the impact of empty and loaded CABVs on the gut microbiome.

Acknowledgements The authors thank Dr. David Craft at Penn State Hershey Medical Center (Hershey, PA) for providing stocks of *E. coli*, *B. fragilis*, and *E. faecalis* used in this work. The authors also thank Ms. Maria Lozoya, M.S. at Midwestern University (Glendale, AZ) for her work with CAB preparations and size distribution measurements.

Funding This project was funded by multi-principal investigator (Drs. Stewart and Sharma) award from the National Institutes of Health, National Institute of Allergy and Infectious Diseases (1R21AI132353-01).

Compliance with ethical standards

Conflict of interest The authors declare that they have no conflict of interest.

References

1. Leffler DA, Lamont JT. *Clostridium difficile* infection. N Engl J Med. 2015;372:1539–48.
2. Zhang S, Palazuelos-Munoz S, Balsells EM, et al. Cost of hospital management of *Clostridium difficile* infection in United States—a meta-analysis and modelling study. BMC Infect Dis. 2016;16:447.
3. Eyre DW, Walker AS, Wyllie D, et al. Predictors of first recurrence of *Clostridium difficile* infection: implications for initial management. Clin Infect Dis. 2012;55:S77–87.
4. Thomas C, Stevenson M, Riley TV. Antibiotics and hospital-acquired *Clostridium difficile*-associated diarrhoea: a systematic review. J Antimicrob Chemother. 2003;51:1339–50.
5. Schubert AM, Rogers MA, Ring C, et al. Microbiome data distinguish patients with Clostridium difficile infection and non-*C. difficile*-associated diarrhea from healthy controls. MBio. 2014;5:e01021–14.
6. Lamendella R, Wright JR, McLimans C, et al. Antibiotic treatments for *Clostridium difficile* infection are associated with distinct bacterial and fungal community structures. mSphere. 2018;3:e00572–17.
7. Daly SM, Sturge CR, Felder-Scott CF, et al. MCR-1 inhibition with peptide-conjugated phosphorodiamidate morpholino oligomers restores sensitivity to polymyxin in escherichia coli. MBio. 2017;8:e01315–17.
8. Otsuka T, Brauer AL, Kirkham C, et al. Antimicrobial activity of antisense peptide-peptide nucleic acid conjugates against nontypeable Haemophilus influenzae in planktonic and biofilm forms. J Antimicrob Chemother. 2017;72:137–44.
9. Hegarty JP, Krzeminski J, Sharma AK, et al. Bolaamphiphile-based nanocomplex delivery of phosphorothioate gapmer antisense oligonucleotides as a treatment for *Clostridium difficile*. Int J Nanomed. 2016;11:3607–19.
10. Stewart DB, Berg A, Hegarty J. Predicting recurrence of *C. difficile* colitis using bacterial virulence factors: binary toxin is the key. J Gastrointest Surg. 2013;17:118–24. discussion p.124-5
11. Ayhan DH, Tamer YT, Akbar M, et al. Sequence-specific targeting of bacterial resistance genes increases antibiotic efficacy. PLoS Biol. 2016;14:e1002552.
12. Howard JJ, Sturge CR, Moustafa DA, et al. Inhibition of pseudomonas aeruginosa by peptide-conjugated phosphorodiamidate

morpholino oligomers. Antimicrob Agents Chemother. 2017;61: e01938–16.
13. Galanakis D, Davis CA, Del Rey Herrero B, et al. Synthesis and structure-activity relationships of dequalinium analogues as K+ channel blockers. Investigations on the role of the charged heterocycle. J Med Chem. 1995;38:595–606.
14. Weissig V, Lasch J, Erdos G, et al. DQAsomes: a novel potential drug and gene delivery system made from Dequalinium. Pharm Res. 1998;15:334–7.
15. Weissig V. From serendipity to mitochondria-targeted nanocarriers. Pharm Res. 2011;28:2657–68.
16. Mileykovskaya E, Dowhan W. Cardiolipin membrane domains in prokaryotes and eukaryotes. Biochim Biophys Acta. 2009;1788:2084–91.
17. Epand RM, Epand RF. Lipid domains in bacterial membranes and the action of antimicrobial agents. Biochim Biophys Acta. 2009;1788:289–94.
18. Marín-Menéndez A, Montis C, Díaz-Calvo T, et al. Antimicrobial nanoplexes meet model bacterial membranes: the key role of Cardiolipin. Sci Rep. 2017;7:41242.
19. Jenior ML, Leslie JL, Young VB, et al. *Clostridium difficile* colonizes alternative nutrient niches during infection across distinct murine gut microbiomes. mSystems. 2017;2:e00063–17.
20. Pepin J. Vancomycin for the treatment of Clostridium difficile infection: for whom is this expensive bullet really magic? Clin Infect Dis. 2008;46:1493–8.
21. McDonald LC, Gerding DN, Johnson S, Bakken JS, Carroll KC, Coffin SE, Dubberke ER, Garey KW, Gould CV, Kelly C, Loo V, Shaklee Sammons J, Sandora TJ, Wilcox MH. Clinical Practice Guidelines for Clostridium difficile infection in adults and children: 2017 update by the Infectious Diseases Society of America (IDSA) and Society for Healthcare Epidemiology of America (SHEA). Clin Infect Dis. 2018;66:987–94.
22. Ajami NJ, Cope JL, Wong MC, Petrosino JF, Chesnel L. Impact of oral fidaxomicin administration on the intestinal microbiota and susceptibility to Clostridium difficile colonization in mice. Antimicrob Agents Chemother. 2018. AAC.02112-17 [Epub ahead of print].
23. Weiss K, Allgren RL, Sellers S. Safety analysis of fidaxomicin in comparison with oral vancomycin for Clostridium difficile infections. Clin Infect Dis. 2012;55(Suppl 2):S110–5.